

## Flexible organic transistors based on solution-sheared PVDF insulator

*S. Georgakopoulos, F.G. del Pozo, M. Mas-Torrent\**

### Supporting information

#### 1. Fabrication

##### 1.1 Gate patterning by photolithography and etching

The substrate used is Polyethylene Terephthalate (PET) coated with Indium Tin Oxide (ITO) (100 nm) (Sigma Aldrich). The protective cover is peeled off and the substrate rinsed with HPLC acetone and isopropanol. A silicon wafer is wetted with a few droplets of isopropanol and the substrate is placed on top. Then the substrate is blown with a stream of nitrogen until no more isopropanol comes out from the edges. The capillary force keeps the substrate flat. Two corners of the substrate are taped on the wafer to prevent delamination at the baking stage. S1813 positive photoresist (Microposit) is spin-coated on the substrate at 4000 RPM, followed by baking at 100°C for 1 min. No HMDS is used in the photolithography process as the adhesion of the photoresist to ITO is sufficient. The photoresist is patterned with a laser writer (Durham magneto-optics) at 405 nm with a dose of 150 mJ/cm<sup>2</sup>. The sample is developed with MF319 developer for 30-60s and rinsed with DI H<sub>2</sub>O. The ITO is etched by immersion into undiluted HCl (30 s), followed by cleaning with DI H<sub>2</sub>O, photoresist removal by acetone, further cleaning with acetone and isopropanol, and drying with a stream of nitrogen.

##### 1.2 PVDF solution shearing

PVDF homopolymer (180,000 g/mol) (Sigma Aldrich) is dissolved in HPLC grade DMF at 10% wt concentration in ambient conditions and heated at 120 °C for several hours for dissolution to occur. A blade coater (ZAA 2300, Zehntner GmbH) with a flat blade applicator (ZUA 2000, Zehntner GmbH) is used to coat the PVDF solution on the substrate. The coating bed of the coater is set to 120°C. The applicator apparatus is left to rest on the hot bed for some time before the deposition and its temperature is assumed to be close to that of the coating bed. It has been previously reported that humidity from the environment has negative effects on the structure and porosity of bar-coated PVDF homopolymer layers<sup>1</sup>. It was reported that this issue is resolved either by exceeding the deposition temperature of 100 °C, or by working in dry atmosphere. In our case the coating is performed in a controlled 25% humidity laboratory. The substrate is 6x6 cm in area and 120µm in thickness, whereas the blade resides at a distance of 1mm from the bed. The planarity of the substrate is critical to achieve uniform deposition of the layer. We have found that the utilization of the capillary force of a liquid between the substrate and the bed works out very well. Glycerine is an ideal choice for this function as it neither reacts with the PET substrate nor evaporates at an appreciable rate at 120°C. Numerous other high boiling point solvents were all found to react and deform the PET at the working temperature. A droplet of glycerine is placed on the bed, and then the substrate is placed on top and blown with a stream of nitrogen until no more glycerine comes out from the sides of the substrate. The PVDF solution vial also resides on the coating bed for some time anterior to the deposition. Approximately 300-500 µL of PVDF solution are placed on the substrate and the applicator moves forward, shearing the solution at a speed of 5 mms<sup>-1</sup>. Higher speeds yield higher PVDF layer roughness in accordance with previous reports<sup>1</sup>. The sample is left on the bed for 2 more minutes to evaporate residual solvent. The sample is picked up carefully to avoid bending, as deformation at this stage will persist after cool down. The sample is placed in a stream of DI H<sub>2</sub>O to remove residual glycerine and dried with a stream of nitrogen.

##### 1.3 Source/Drain photolithography

The sample is placed on a silicon wafer utilising isopropanol to improve adhesion as described in section 1.1. Photoresist is deposited and baked as described in section 1.1. ITO alignment markers along the periphery of the sample are exposed by scratching off the PVDF/photoresist layers. The exposure dose required

was  $150 \text{ mJcm}^{-2}$ , however this dose is high and results in the formation of bubbles of the underlying PVDF layer (localised delamination in the S/D electrode area). The issue is fully resolved by performing two passes of  $75 \text{ mJcm}^{-2}$  (same total intensity but lower exposure rate). Although the double pass is utilised, it is noted that the bubbles formed in the one-step writing process have no effect whatsoever on electrical performance. The sample is developed as described in section 1.1. Cr is evaporated at a rate of  $0.2 \text{ \AA/s}$  with 5 nm total thickness. Au is evaporated initially at a rate of  $0.1 \text{ \AA/s}$  and after several nanometers at  $0.5 \text{ \AA/s}$ , with 35 nm total thickness (monitored by a pre-calibrated quartz crystal microbalance). The support on which the sample is located is water-cooled and good contact is essential for lift-off to work; if the photoresist is heated excessively it becomes insoluble. Lift-off was performed by immersing the samples in ethanol. Note that lift-off is commonly performed with acetone, but due to its high vapour pressure it causes complete delamination of the PVDF from the ITO/PET. Samples are cleaned with additional HPLC ethanol and dried with a stream of nitrogen.

#### **1.4 Argon plasma etching for improved surface wetting**

The samples are subsequently placed in a RIE 2000 CE (South Bay technologies) at 100 mTorr Ar, 50 W for 30s. Shorter exposure times can work (10 s) but higher OFET parameter spread was observed.

#### **1.5 DB-TTF:PS solution shearing**

DB-TTF is purchased from Sigma Aldrich and used without further purification. This material is blended with polystyrene ( $3000 \text{ gmol}^{-1}$ ) in a ratio of 1:3 in 4% wt in anhydrous chlorobenzene and the resulting solution is heated at  $105^\circ\text{C}$ . The solution is also placed on the hot coater bed (same temperature) before deposition. Different blending ratios of DBTTF and PS had a weak influence on the device performance. A mean OFET mobility of approximately  $0.1 \text{ cm}^2/\text{Vs}$  was measured for both 1:2 and 1:4 ratio blends, versus  $0.2 \text{ cm}^2/\text{Vs}$  for the 1:3 blend.

The sample is placed on a coater bed (RK print) at  $105^\circ\text{C}$  (utilizing glycerine as described in section 1.2), and a smooth bar located 0.3 mm above the sample shears the solution forward at a speed of  $10 \text{ mms}^{-1}$ , as previously reported.<sup>2</sup> The sample is removed immediately as prolonged heating at this temperature significantly degrades the device performance.. The samples are rinsed with DI  $\text{H}_2\text{O}$ , dried with a stream of nitrogen and placed in an oven at  $60^\circ\text{C}$  and 10% relative humidity for two hours.

## **2. Additional experimental details and data**

### **2.1 Profilometry**

Profilometry measurements were performed on a P16+ profilometer (KLA Tencor). The measured thickness of the PVDF layer was  $1000 \pm 25 \text{ nm}$ .

## 2.2 PVDF FTIR

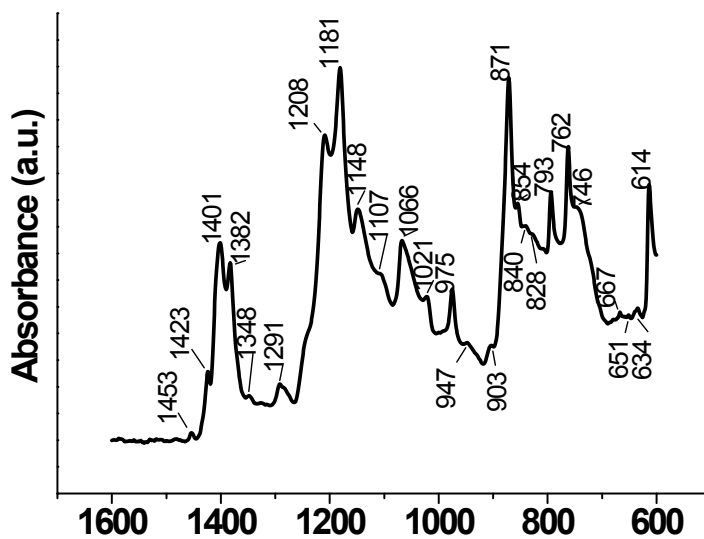


Figure S1. FTIR spectrum of PVDF thin film surface.

FTIR measurements were carried out with a Perkin Elmer Spectrum One. 20 scans were averaged. The PVDF thin films were measured before and after exposure to Ar plasma and no clear differences were observed.

## 2.3 PVDF capacitance

Capacitance measurements were performed with a Novocontrol Alpha-A analyser and a ZG4 interface connected to two EverBeing EB-700VL probes. The capacitance was extracted assuming a series resistance equivalent circuit.

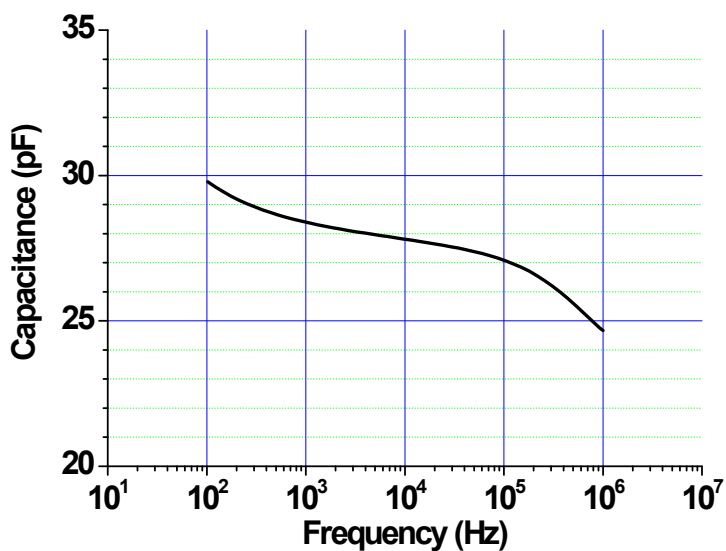


Figure S2. Capacitance of an ITO/PVDF/Cr/Au capacitor of area  $0.41 \cdot 10^{-6} \text{ m}^2$  measured over a range of frequencies.

## 2.4 Electrical characterisation

Electrical characterisation was performed with an Agilent B1500A. OFETs and inverters were measured with HR – PLC 1 integration time settings corresponding to an integration time of 20ms per measured data point.

Charge carrier mobility was extracted in the saturation regime with the following equation:

$$\mu_{SAT} = \left( \frac{d\sqrt{I_D}}{dV_G} \right)^2 \frac{2L}{C_i W}$$

Extracted values are peak values of a linearly decreasing mobility profile with increasing negative gate voltage.

## 2.5 AFM

AFM measurements were performed with an Agilent 5100 in tapping mode. FORT tips (AppNano) with 6 nm radius were used.

## 2.6 XRD

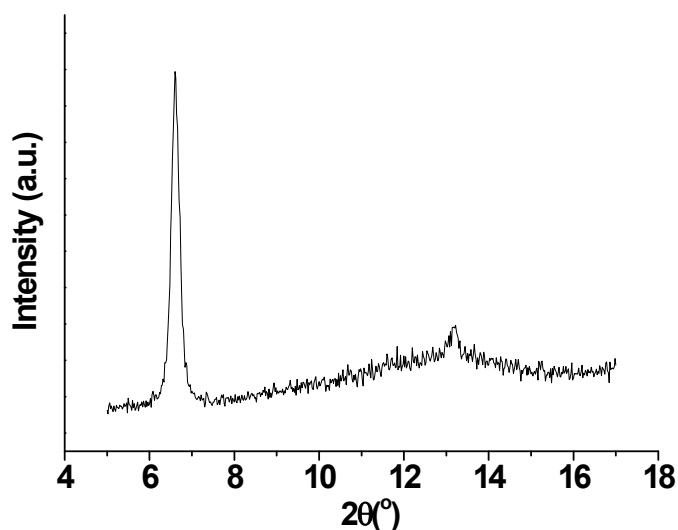


Figure S3. Normal angle XRD spectrum of finished OFET structure. The two observable peaks are characteristic of  $\gamma$ -phase DBTTF.

XRD measurements were performed with a Siemens D-5000, using a Cu anode scintillation detector.

## 2.7 XPS

XPS measurements were performed with a Phoibos 150 analyzer (SPECS GmbH, Berlin, Germany) in ultra-high vacuum conditions (base pressure  $5 \cdot 10^{-10}$  mbar) with a monochromatic aluminium K $\alpha$  x-ray source (1486.74 eV). The energy resolution measured by the FWHM of the Ag 3d $_{5/2}$  peak for a sputtered silver foil was 0.6 eV. The spot size was 3.5 mm by 0.5 mm. For the estimation of the penetration the following relation was used:

$$d = 3\lambda \cos(\theta)$$

where  $d$  is the estimated thickness,  $\theta$  the angle, and  $\lambda$  the inelastic mean free path. The  $\lambda$  value of glassy carbon was used which should be a close approximation to the organic active layer used in this work.

## 2.8 Bending

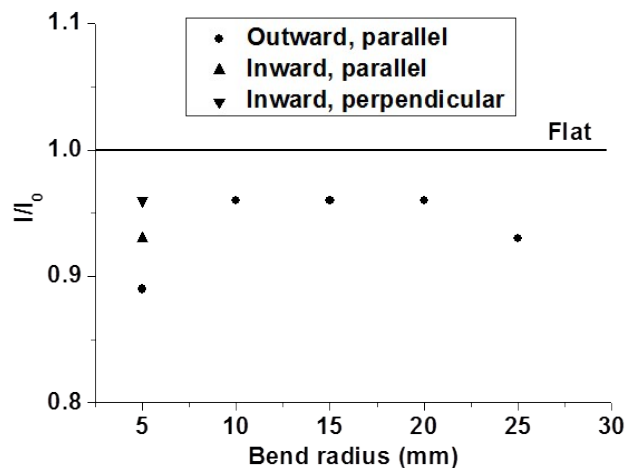


Figure S4. For bending measurements, the substrate was attached onto a flexible metal sheet, which was bent inwards or outwards to the desired radius, with the bending direction parallel or perpendicular to the OFET channels. The transfer characteristics were measured and the current at  $V_G=V_D=-40$  V was extracted from each measurement and plotted against bend radius (a). The line at  $I/I_0=1$  corresponds to the current value extracted from the flat sample.

## 2.9 Inverter

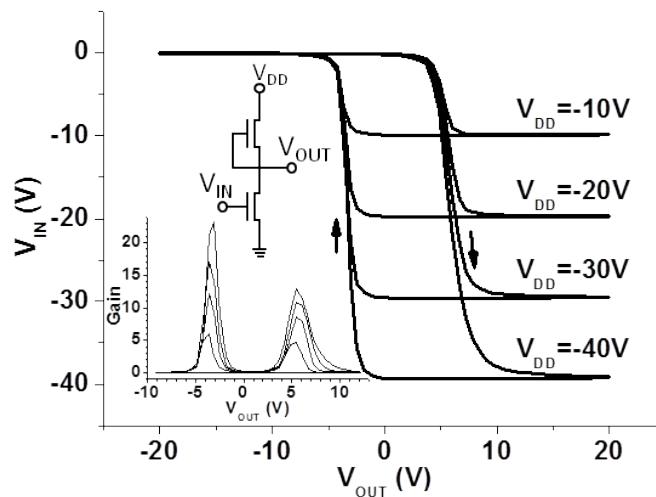


Figure S5. Unipolar inverter characteristic. The drive/load OFET width ratio is 1:1. Channel dimensions are  $L=50$   $\mu\text{m}$ ,  $W=4$  mm.

<sup>1</sup> M. Li, I. Katsouras, C. Piliago, G. Glasser, I. Lieberwirth, P. W. M. Blom, D. M. de Leeuw. *J. Mater. Chem. C*, 1, 7695 (2013)

<sup>2</sup> F. G. del Pozo, S. Fabiano, R. Pfattner, S. Georgakopoulos, G. Galindo, X. Liu, S. Braun, M. Fahlman, J. Veciana,

---

X. Crispin, M. Berggren, M. Mas-Torrent, *Adv. Funct. Mater.* 2015, 10.1002/adfm.201502274.